

# Boosting Scientific Error-Bounded Lossy Compression through Optimized Synergistic Lossy-Lossless Orchestration

Shixun Wu\*  
University of California,  
Riverside  
United States  
swu264@ucr.edu

Jinwen Pan\*  
Technical University of  
Munich  
Germany  
jinwen.pan@tum.de

Jinyang Liu†  
University of Houston  
Houston, TX, United  
States  
jliu107@uh.edu

Giannan Tian  
University of Kentucky  
United States  
giannan.tian@uky.edu

Ziwei Qiu  
University of Houston  
Houston, TX, United  
States  
zqiu4@cougarnet.uh.edu

Jiajun Huang  
University of South  
Florida  
United States  
jiajunhuang@usf.edu

Kai Zhao  
Florida State University  
Tallahassee, FL, USA  
kai.zhao@fsu.edu

Xin Liang  
University of Kentucky  
Lexington, KY, USA  
xliang@uky.edu

Sheng Di  
Argonne National  
Laboratory  
Lemont, IL, USA  
sdi1@anl.gov

Zizhong Chen  
University of California,  
Riverside  
United States  
chen@cs.ucr.edu

Franck Cappello  
Argonne National  
Laboratory  
Lemont, IL, USA  
cappello@mcs.anl.gov

## Abstract

As high-performance computing architectures evolve, more scientific computing workflows are being deployed on advanced computing platforms such as GPUs. These workflows can produce raw data at extremely high throughputs, requiring urgent high-ratio and low-latency error-bounded data compression solutions. In this paper, we propose **cuSZ-Hi**, an optimized high-ratio GPU-based scientific error-bounded lossy compressor with a flexible, domain-irrelevant, and fully open-source framework design. Our novel contributions are: 1) We maximally optimize the parallelized interpolation-based data prediction scheme on GPUs, enabling the full functionalities of interpolation-based scientific data prediction that are adaptive to diverse data characteristics; 2) We thoroughly explore and investigate lossless data encoding techniques, then craft and incorporate the best-fit lossless encoding pipelines for maximizing the compression ratio of cuSZ-Hi; 3) We systematically evaluate cuSZ-Hi on benchmarking datasets together with representative baselines. Compared to existing state-of-the-art scientific lossy compressors, with comparative or better throughput than existing high-ratio scientific error-bounded lossy compressors on GPUs, cuSZ-Hi can achieve up to 249% compression ratio improvement under the same error bound, and up to 215% compression ratio improvement under the same decompression data PSNR.

## 1 Introduction

No doubt that we are in the exascale computing era, in which today’s scientific applications tend to be running on extremely large-scale environments, continuously producing

masses of scientific data. The world’s best exascale supercomputers, like Frontier [4], Aurora [6], and El Capitan [5], which present peak performances around or over 1 Exaflops, have pushed the scientific computational power to a brand new magnitude, which is highly attributed to the cutting-edge GPU hardware that those supercomputers facilitate. Correspondingly, exascale scientific computing workflows have been established on GPU platforms, which include diverse scientific domains such as cosmology [39], turbulence [46], and molecular dynamics [10]. However, higher computational power always leads to higher data generation speed, and the development of scientific computing workflows on GPU platforms is in great need of more effective data management solutions, which are critical to the storage, analysis, and transmission of exascale scientific data. For example, in [46], a GPU-accelerated turbulence simulation framework is proposed, which can generate data grids of 35 trillion grid points (128 TB in single-precision). To this end, effective scientific data reduction techniques are required to be available on GPU platforms to relieve the system bottleneck in I/O and storage with relatively low latency. The error-bounded lossy compression of scientific data can greatly reduce the data volume while preserving the per-data accuracy well, so it is commonly regarded as the best-fit data reduction solution for scientific data [29, 30, 43, 45, 51].

Over the past years, there have been various practices and deliverables of GPU-based scientific error-bounded lossy compression, which project substantial potential in integrating them into GPU-based scientific computing workflows. For example, cuSZ [36, 44, 45] and cuZFP [13, 30] have been leveraged by existing scientific applications, and cuSZp [20, 21] is an excellent high-throughput data compressor to be leveraged in performance-favored GPU data compression. Nevertheless,

\*Both authors contributed equally to this research.

†Corresponding author: Jinyang Liu, Department of Computer Science, University of Houston, Houston, TX 77204.

a significant research gap remains in this field: **An open-source design for high-ratio scientific error-bounded lossy compression on GPUs is still missing.** Most existing works focus on high throughput, relying on low-cost and low-quality data processing algorithms. cuSZ-I [36], as the first and the only existing GPU-based high-ratio-and-quality scientific data compressor, integrates an NVIDIA-proprietary lossless encoding module to achieve a compression ratio higher than 32, yet still exhibits much lower compression ratio than CPU-based compressors, like SZ3 [29] and QoZ [29, 34]. The most critical challenges of high-ratio scientific error-bounded lossy compression on GPU platforms are: 1) It is non-trivial to propose effective GPU-parallelization models and practical high-throughput implementations of high-ratio scientific data compression algorithms; 2) To optimize the GPU-based high-ratio scientific lossy compression pipelines, a thorough and in-depth benchmarking and analysis on the data decomposition and encoding modules on GPU platforms are required.

In this paper, committing to optimizing high-ratio scientific error-bounded lossy compression on GPU platforms, we propose cuSZ-Hi, which is a general, open-source, and highly effective solution. From the decomposition-encoding perspective of error-bounded lossy compression, based on the prior success of interpolation-based error-bounded lossy compressors [33, 34, 36, 50], we fine-craft a well-rounded GPU-parallelized interpolation-based data predictor, which is oriented from maximizing the lossless compressibility of integer decomposition data. Furthermore, from systematic investigation, evaluation, and benchmarking on GPU-based numerical lossless encoders, we establish the best lossless pipelines for cuSZ-Hi, which fully leverages different aspects of redundancy information in the data, ensuring the high-magnitude compression ratio among all use cases. Our contributions are as follows:

- In cuSZ-Hi, we further optimize the high-throughput interpolation-based data prediction on GPU platforms, proposing a new scientific data prediction module with multiple interpolation schemes and auto-tuned configurations;
- After an in-depth investigation of existing numerical lossless encoders, we craft and incorporate the best-fit lossless encoding pipelines for maximizing the compression ratio of cuSZ-Hi.
- We perform a comprehensive evaluation of cuSZ-Hi on 6 real-world scientific datasets. cuSZ-Hi exhibits outperforming compression ratio and quality compared to all existing state-of-the-arts. cuSZ-Hi can achieve up to 249% compression ratio improvement over existing scientific lossy compressors under the same error bound and up to 215% compression ratio improvement under the same decompression data PSNR.

We organize the rest of this paper as follows: Section 2 discusses the related work of this paper. Section 3 formulates our research target and the background of interpolation-based scientific error-bounded lossy compression on GPUs. In Section 4, we propose the framework design and module composition of cuSZ-Hi. Section 5 demonstrates our detailed

designs for optimizing cuSZ-Hi. In Section 6, we present the evaluations for cuSZ-Hi. Section 7 concludes this work and discusses future plans.

## 2 Related Work

### 2.1 Scientific error-bounded lossy compression

Error-bounded lossy compression has been regarded as the best-fit strategy for scientific data size reduction. Existing error-bounded lossy compressors have proposed diverse technical solutions, and present different capabilities on use cases and metrics. Among the most representative works, SZ-family [29, 33, 34, 52] follows a hybrid design of spline interpolation [50], Linear Regression, and Lorenzo extrapolation [42]. ZFP [30] and SPERR [26] proceed data with transforms and specialized encoding schemes. TTHRESH [9] leverages high-order singular value decomposition to effectively de-correlate the input data. To maximally reduce the compressed data size, there are various deep-learning-integrated frameworks for scientific error-bounded lossy compression [17, 19, 27, 31, 32, 37, 38]. To optimize the compression throughput, compressors like SZx [47] and SZp (FZ-light) [18] reduce their lossy data processing scheme to very-simplified offset-computation and bit-analysis.

### 2.2 Error-bounded lossy compression on GPUs

Based on the aforementioned scientific error-bounded lossy compression frameworks, several GPU-based scientific lossy compressors have been proposed for several purposes: (1) They can deliver much higher magnitudes of data throughput than CPU-based compressors; (2) They can be directly integrated into existing and emerging scientific computing applications on GPU platforms with little system latency and overhead. Several examples are:

- **cuSZ:** cuSZ [36, 44, 45] was proposed in 2020, revised in 2021, and updated in 2024. The latest version of cuSZ merges the recently proposed cuSZ-I [36] and the original Lorenzo-based cuSZ [44, 45]. It integrates 2 data predictors (Lorenzo predictor and interpolation predictor), then applies Huffman encoding (and also an optional NVIDIA Bitcomp) as the lossless module.
- **cuSZp2:** cuSZp2 [20] is an end-to-end performance optimized scientific error-bounded lossy compressor on GPU platforms. It leverages 1D offset prediction and fix-length encoding for high-speed scientific data compression.
- **cuZFP:** cuZFP [13, 30] performs scientific error-bounded lossy compression with discrete orthogonal transform and embedding encoding. It has a balanced compression ratio and throughput.
- **FZGPU:** Derived from cuSZ, FZGPU alters the compression pipeline by replacing the lossless encoding stage with bit-shuffle and dictionary encoding, aiming to deliver higher throughput.
- **Others:** cuSZx [47] features a monolithic design to deliver extremely high throughput at the cost of lower data quality and compression ratio. MGARD-GPU [16] is another GPU

compressor practice based on the MGARD compression algorithm [7].

### 2.3 Lossless encoding in scientific lossy compression

In the past years, lossless compression (encoding) techniques have not only served as standalone data compressors but have also been widely adopted by scientific error-bounded lossy compressors to improve data reduction rates [35]. From gzip [14] in SZ1.0, Zstd [12] in SZ3, SPECK [40] in SPERR, to NVIDIA Bitcomp in cuSZ-I [36], diverse lossless encoders have enhanced the scientific error-bounded lossy compression. Among those encoders, there are entropy-based encoders that compress the data by token frequency information (such as Huffman encoding), redundancy-based encoders that compress the data by reducing repeat patterns (such as run-length encoding), and a mixture of those 2 techniques (such as Zstd, Deflate [15], etc.). On GPU platforms, there are also multiple open-source and proprietary lossless encoders for scientific numerical data [11], including but not limited to GPULZ [49], ndzip [25], and nvCOMP [2]. The recently developed LC framework [8] integrates over 10 long-standing components (e.g., mutators, shufflers, reducers) used in constructing lossless compressors, supporting various symbol widths. This framework enables users to traverse diverse component combinations for the files requiring compression and customize compressors with an arbitrary number of stages at a fine-grained level while supporting heterogeneous compression/decompression across GPUs and CPUs.

## 3 Research Background

### 3.1 Problem formulation of scientific error-bounded lossy compression

We mathematically formulate our research problem: scientific error-bounded lossy compression on GPU platforms. Generally, given an input scientific data  $X = \{x_i\}$ , a pair of compressor and decompressor  $\text{Cmp}, \text{Dec}$  converts  $X$  to compressed data  $Z = \text{Cmp}X$  and decompressed data  $X' = \{x'_i\} = \text{Dec}Z$ . The optimization of the compression ratio, which is defined by the input data size divided by the compressed data size, is described as follows:

$$\begin{aligned} & \text{Maximize } \frac{|X|}{|Z|} \\ & \text{s.t. } Z = \text{Cmp}X, X' = \text{Dec}Z \\ & \text{and } \|X - X'\|_\infty = \max |x_i - x'_i| \leq \epsilon \end{aligned} \quad (1)$$

In Eq. 1, the upper bound of point-wise data error  $\epsilon$  is named the error bound in the compression task. We further specify this problem in 2 aspects: 1) Regarding the GPU-based error-bounded lossy compression, the whole compression pipeline should be highly parallelized on the hardware, presenting high computing throughputs (often ten or hundreds of Giga-bytes of data per second in modern platforms); 2) We observe that scientific error-bounded lossy compressors mostly follow a framework design of lossy decomposition plus lossless

encoding (detailed in Section 4). The input floating-point data is first lossy decomposed to integer data with high compressibility, and the integers are further lossless encoded to gain size reduction. Eq. 2 involves this framework scheme, formulating our research target. We would like to jointly optimize the integer decomposition process (Dcp) and the lossless encoding (Enc) process while preserving the required computing throughput ( $\text{SpeedDcp}, \text{Enc}$ ) with speed higher than a threshold  $S_t$  (we initially set it to a comparable speed to cuSZ-I):

$$\begin{aligned} & \text{Dcp, Enc} = \arg \max_{\text{Dcp, Enc}} \frac{|X|}{|\text{EncDcp} X|} \\ & \text{s.t. } \|X - X'\|_\infty = \max |x_i - x'_i| \leq \epsilon \\ & \text{and } \text{SpeedDcp, Enc} \geq S_t \end{aligned} \quad (2)$$

### 3.2 Interpolation-based error-bounded lossy compression on GPUs

In this subsection, we introduce the interpolation-based error-bounded lossy compression on GPUs (specifically cuSZ-I [36]) as our research background, as cuSZ-Hi also integrates an interpolation-based data predictor. The core design of cuSZ-I is illustrated in Figure 1. To ensure parallelization, cuSZ-I partitions the input data into small chunks (e.g.,  $33 \times 9 \times 9$  for 3D data), each composed of 4 basic blocks (shown in Figure 1), and allocates each chunk to a thread block. Leveraging spline interpolations, a thread block predicts the allocated data chunk from a losslessly stored sparse anchor grid (in the stride of 8 on each dimension) and then quantizes the prediction errors to integers for the subsequent lossless size reduction process. The interpolations follow a hierarchical scheme, performing interpolation in different sequential steps, from high levels (with large interpolation strides) to low levels (with small interpolation strides) along all dimensions. The computations are fully parallelized on the threads within each interpolation level and dimension. After acquiring the quantized integer errors (a.k.a. the quantization codes), cuSZ-I applies Huffman encoding and an optional proprietary NVIDIA Bitcomp [2] lossless compression module to finalize the size reduction.

cuSZ-I (especially its Bitcomp-integrated version) has achieved state-of-the-art compression ratio and data quality in GPU-based scientific error-bounded lossy compression. In this paper, we will keep focusing our compressor design on interpolation and integer encoding techniques due to the unique potential of interpolation in proposing high-accuracy data predictions with relatively low computational costs. Furthermore, we will address several existing critical limitations of interpolation-based scientific data compression on GPUs, including but not limited to 1) suboptimal data-partition and anchor-sampling strategy; 2) outdated design of interpolation process and its auto-optimization; 3) lacking effective and open-source lossless encoding solution for quantized errors.

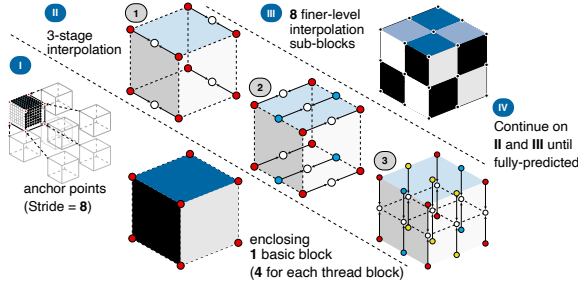


Figure 1: Design overview of cuSZ-I (interpolation-based scientific error-bounded lossy compression on GPUs).

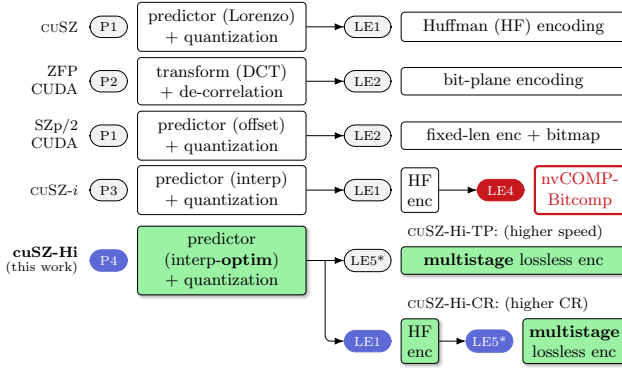


Figure 2: Decomposition-encoding-based framework design of cuSZ-Hi, compared to existing works.

#### 4 The Framework Design of cuSZ-Hi

The compression framework design of cuSZ-Hi is proposed in Figure 2, comparing it to other existing representative GPU-based scientific error-bounded lossy compressors. Although those compressors have diverse compression framework designs, they all share a uniform scheme, which is lossy data decomposition and lossless integer encoding, as shown in Figure 2. The first module of each framework de-correlates the input floating point data, producing integers as intermediate results. Those integers have higher compressibility than the original input, contain reduced information but preserve the error bound, and are generated by different data processing techniques such as direct value quantization (in cuSZp2), Lorenzo extrapolation (in cuSZ), and spline interpolation (in cuSZ-I). Afterward, the lossless encoding modules in each compressor reduce the size of the intermediate integers with no information loss so that the final output can serve as the error-bounded compression result. We detail the framework modules of cuSZ-Hi as follows and explain why they bring an optimized design regarding compression ratio and quality.

- **Lossy data decomposition:** cuSZ-Hi adopts spline-interpolation-based data prediction, which features an advanced design over the predictor in cuSZ-I [36]. Spline-interpolation-based data prediction has been proven to be the best-fit data decomposition technique for scientific error-bounded lossy compression because it can achieve both high data prediction accuracy and computation speed [33, 34, 36, 50]. In

contrast, compressors with other lossy decomposition techniques, such as cuSZ, cuSZp2, and cuZFP, suffer from a significantly lower compression ratio than cuSZ-I. Based on the high-throughput parallelized implementation of spline interpolations proposed by [36], cuSZ-Hi further tune and optimize the GPU-based spline interpolation design to maximize the compression ratio acquired.

- **Lossless integer encoding:** To maximize the compression ratio, a well-rounded lossless encoding pipeline is necessary, which should be able to leverage the data correlation information on both token-level and bit-level. Unfortunately, among existing compressors, cuSZ only integrates the frequency-based Huffman encoding and cuSZp2/cuZFP merely applies fix-length bit-wise de-redundancy encodings. cuSZ-I managed to combine both Huffman encoding and de-redundancy encoder, but the NVIDIA Bitcomp module it leverages is a proprietary product with limited usability. In cuSZ-Hi, after synthetically investigating and benchmarking available lossless encoding solutions, cuSZ-Hi proposes new open-source lossless pipelines that jointly facilitate Huffman encoding and high-performance multi-stage lossless modules. Moreover, as indicated in Figure 2, cuSZ-Hi integrates 2 different lossless pipelines, which can be flexibly selected according to the user’s requirements, presenting a higher compression ratio (in **cuSZ-Hi-CR** mode) or throughput (in **cuSZ-Hi-TP** mode).

#### 5 Synergistic Lossy-Lossless Module Design

As Figure 2 indicates, optimizing the floating data compression ratio of scientific error-bounded lossy compression pipelines is equivalent to improving the compression for the “lossy decomposed” integer array (in cuSZ-Hi, it is the array of quantized predictor errors). To this end, there are two different but synergistic solutions: Increasing the compressibility of the integer array and promoting the capability of lossless integer encoding modules. In this section, we will detail our new GPU-based compression module designs regarding those 2 methodologies.

##### 5.1 Improving interpolation-based lossy data prediction

Because lossless data encoding algorithms mainly leverage 2 types of data information: token-wise entropy and bit-wise redundancy, there are also 2 direct solutions for improving the compressibility of quantization codes from the cuSZ-Hi interpolation-based data predictor. First, we present better data prediction accuracy and anchor-point rate, making the distribution of quantization codes more concentrated to zero, delivering lower entropy. Second, based on the characteristics of interpolation-based data predictors, we reorder the quantization code array with a fixed mapping, bringing similar values together to raise its compressibility.

**5.1.1 Reorganized data and anchor partitions.** In Figure 3, we present the details of cuSZ-Hi thread-block-wise data partition, anchor layout, and interpolation workloads in a 3D

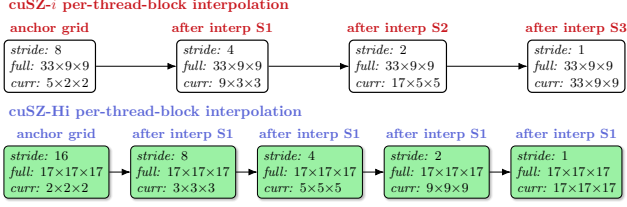


**Figure 3: Per-thread-block anchor and interpolation partition in cuSZ-I and cuSZ-Hi on 3D data.**

example, comparing it to cuSZ-I. Specifically: 1) In cuSZ-Hi, the 3D partitioned data block to be processed by each thread block has a size of  $17^3$  (including all anchors) instead of  $33 \times 9 \times 9$  for cuSZ-I. 2) On each dimension, the stride of losslessly stored anchor points is 16 in cuSZ-Hi instead of 8 in cuSZ-I. Due to this, the interpolations for 3D data blocks in cuSZ-Hi follow a 4-level hierarchy instead of the cuSZ-I 3-level interpolation. We justify our new design as follows: First, a dimensionally isotropic data partition can be better adaptive to different interpolation computation orders, which will be detailed in Section 5.1.4. Second, the data block size in cuSZ-Hi is double the original data block size in cuSZ-I, which better exploits the shared memory and cache in GPU architectures and brings more available data points in the prediction process for improving the data prediction accuracy [34]. Moreover, in our preliminary experiments, further enlarging the data block will bring limited compression ratio improvement while significantly reducing the compression speed. Last, according to preliminary experiments, anchor points in cuSZ-I occupy a considerable portion of the compression data size. Reducing the number of anchor points (to  $\frac{1}{8}$  of cuSZ-I) can effectively reduce the anchor storage overhead meanwhile preserving the data prediction quality.

**5.1.2 Parallelized multi-dimensional interpolation.** Regarding the GPU-parallelized design of interpolation-based data prediction, cuSZ-Hi also introduces a new scheme, which is featured in Figure 4. To further leverage the data correlation along multiple data dimensions, adopting the design concepts proposed in [34], cuSZ-Hi crafts a new parallelized, multi-dimensional-interpolation-based prediction scheme in each partitioned data block (Figure 4 (b)). Unlike original 1D interpolation dimension sequences ((Figure 4 (a))), on each level, parallelized multi-dimensional interpolations follow a process with an increasing number of dimensions used in the interpolation ( $1D \rightarrow 2D \rightarrow 3D$ ). This scheme is isotropic along all dimensions (so free of dimension sequence selection) and better leverages the multi-dimensional data correlation than the existing one-dimensional spline interpolation scheme. In predicting one certain data point along multiple dimensions, the prediction value is the interpolation-prediction average along those dimensions. Moreover, to improve the prediction quality, only prediction values with the highest spline order will be used and averaged in the prediction. For example, two cubic spline interpolations along two dimensions in cuSZ-Hi will be averaged as the final data prediction, but if one is

cubic and the other is linear/quadratic, cuSZ-Hi will only use the cubic spline interpolation as the prediction result.

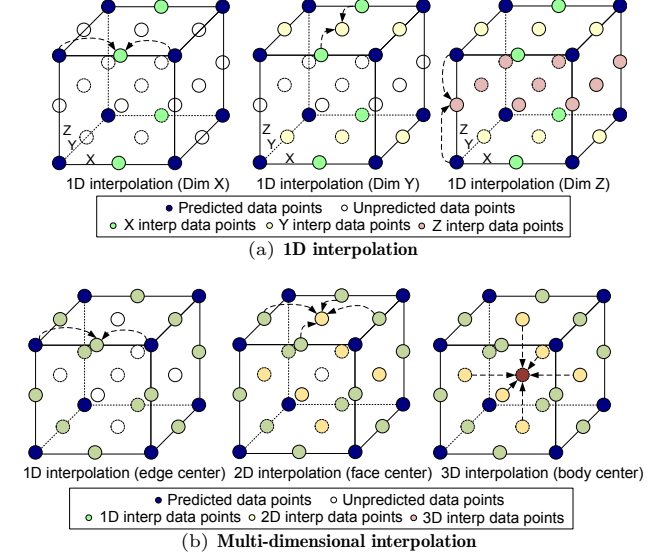


**Figure 4: GPU-based multi-dimensional interpolation (v.s. 1D interpolation). Interpolations for data points in the same colors are fully parallelized.**

**5.1.3 Workload-balanced auto-tuning.** cuSZ-Hi introduced multiple interpolation splines and schemes, which adapt differently to input data characteristics. To this end, an on-line dynamic selection of those splines and schemes will be critical in optimizing the compression ratio of cuSZ-Hi on diverse data inputs. Previously, cuSZ-I merely conducted fast profiling on sampled input data points to determine the best-fit interpolation spline and scheme, which is insufficient to make an accurate selection for interpolation configuration. Following the design proposed in [33, 34], the compression pipeline of cuSZ-Hi includes a full-functional module of interpolation auto-tuning, which is still lightweight enough, with well-balanced workloads on thread blocks to minimize the overhead in GPU-parallelized compression computing. Specifically, cuSZ-Hi first uniformly samples data blocks (with the same size as per-thread-block-data), with a total volume of 0.2% of the whole data. In the auto-tuning kernel, each sampled data block is distributed to multiple thread blocks to perform interpolations on different levels with different splines and schemes.

To optimize the performance of the auto-tuning kernel, best balancing the number of thread blocks used and per-block workload, cuSZ-Hi manages the interpolation test differently on different levels. For level 4 and level 3 interpolations, which have limited computational cost, interpolation tests with all possible configurations (spline scheme) are performed on the same threadblock. For level 2 interpolation, the tests are equally allocated to 2 thread blocks. For level 1 interpolation, which requires intensive computation, cuSZ-Hi leverages 6 thread blocks to test one configuration on each.

After performing the interpolation tests on each level and with each configuration, cuSZ-Hi collects the aggregated data prediction errors from each test and selects the interpolation configuration separately on each level that has the minimized test error.

**5.1.4 Mapping-based quantization codes reordering.** The Huffman encoding module (which is adopted by SZ3, cuSZ, and cuSZ-I) is entropy-based, which means that its compression ratios on lossy-predicted quantization codes are solely dependent on the frequency distribution of the tokens (i.e., values of the codes). However, it cannot exploit the sequential order of the tokens and the bit-wise redundancies in the tokens. To this end, cuSZ-Hi incorporates additional bitwise-redundancy-based lossless encoding modules (detailed in Section 5.2), and the quantization codes are also reversibly reordered to optimize the de-redundancy encoding.

As previously mentioned, in cuSZ-Hi, the data predictions are performed by spline interpolations with diverse strides. For example, data points whose coordinates have at least one odd value are predicted by interpolation with stride 1, and the rest of the data are predicted by interpolations with larger strides (2 to 8). In existing cuSZ-I, the quantized prediction errors are gathered in an array that has the same layout as the input data, and the coordinates of each element remain the same as the corresponding input data point. Therefore, when the quantization code array is flattened to a 1D sequence for lossless encoding, the quantization codes from different interpolation levels and strides will get shuffled in the sequence. However, several existing research works [33, 34, 36] have observed and proved that the prediction accuracy of interpolation-based data predictor is highly relevant to the interpolation stride, for which larger interpolation strides lead to higher data prediction errors. Therefore, quantization codes from large-stride interpolations often present larger absolute values and exhibit different distributions from quantization codes generated by small-stride interpolations. Those insights into the distribution of the quantization codes drive us to rearrange the to-be-encoded quantization code sequence by separating quantization codes from different interpolation strides.

Specifically, after acquiring the multi-dimension quantization code array (the coordinates are the same as the data array), cuSZ-Hi maps the array to a reordered 1D sequence for lossless encoding, in which quantization codes for each interpolation level are grouped in adjacent indices. For example, for a quantization code with coordinate  $x, y, z$  in the 3D code array, its index  $l x, y, z$  in the mapped 1D sequence will be ( $A$  is the stride of anchor points, like 16,  $d_x, d_y, d_z$  are the global data dimension sizes):

$$\begin{aligned}
 l x, y, z &= \text{Prefix} l \ x d_x d_z \ y d_z \ z \\
 &= \left\lfloor \frac{x}{2} \right\rfloor \left\lfloor \frac{d_y}{2} \right\rfloor \left\lfloor \frac{d_z}{2} \right\rfloor - \mathbf{1}_{\{x \text{ even}\}} \left\lfloor \frac{y}{2} \right\rfloor \left\lfloor \frac{d_z}{2} \right\rfloor - \mathbf{1}_{\{x, y \text{ even}\}} \left\lfloor \frac{z}{2} \right\rfloor \\
 l &= \max \left\{ l \in \mathbb{N}, 0 \leq l \leq \log_2 A, 2^l | x, y, z \right\}, \\
 \text{Prefix} l &= f_x l f_y l f_z l \ l < \log_2 A, \text{Prefix} l = 0 \ l = \log_2 A, \\
 f_x 0 &= \left\lfloor \frac{d_x}{2} \right\rfloor, f_y 0 = \left\lfloor \frac{d_y}{2} \right\rfloor, f_z 0 = \left\lfloor \frac{d_z}{2} \right\rfloor, \\
 f_x k \ 1 &= \left\lfloor \frac{f_x k}{2} \right\rfloor, f_y k \ 1 = \left\lfloor \frac{f_y k}{2} \right\rfloor, f_z k \ 1 = \left\lfloor \frac{f_z k}{2} \right\rfloor
 \end{aligned} \tag{3}$$

In Eq. 3,  $l$  indicates the interpolation level for predicting the data point with coordinate  $x, y, z$ , and  $\text{Prefix} l$  is the number of data points on higher interpolation levels. According to Eq. 3, quantization codes from the larger interpolation strides will appear first in the 1D code sequence (with smaller sequence index  $l x, y, z$ ), followed by codes from smaller interpolation strides. In Figure 5, we present the distribution of quantization code values by indices in the code sequences, both from direct flattening and cuSZ-Hi reordering. In the non-reordered code sequence, the code values oscillate intensively over a wide range. Quantization code reordering transfers most outlier values to a short range (beginning of the sequence), highly increasing the overall smoothness of the sequence to improve the compression ratio.

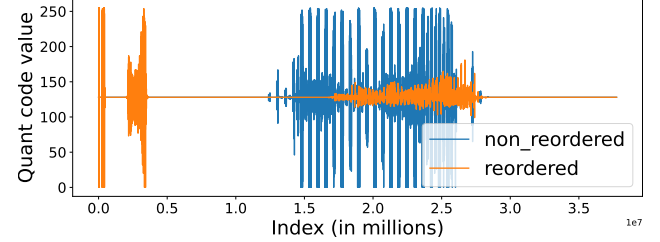


**Figure 5: Comparison between original and reordered quantization code sequences (from compressing Miranda-Pressure data snapshot with error bound  $\epsilon = 1e-3$ ).**

## 5.2 Optimizing lossless ratio and throughput

Past research over years [35, 44] and recently proposed [8, 11] have proved that the evolving lossless data encoding techniques have great potential in improving the scientific lossy compression over various aspects, including both compression ratio and throughput. According to existing work [36] and our investigation, one fact lies in our findings: **Multiple existing scientific lossy compressors have not fully utilized the correlation information in the original data, leaving undealt compressibilities in the output data.** In Table 1, we present a showcase, listing the lossless compression ratio by NVIDIA Bitcomp [2] of several compressed outputs from scientific error-bounded lossy compressors, including base-lines (detailed in Section 2 and Section 6.1) and our proposed cuSZ-Hi. Most of the compression outputs can still be highly compressed by NVIDIA Bitcomp, to 10% ~ 40% of the original sizes, and this is just the reason why cuSZ-I directly



integrated NVIDIA Bitcomp as a module of its pipeline. Unfortunately, Bitcomp is NVIDIA-proprietary, so integrating it into the compression framework will bring severe restrictions on its extension, customization, and (cross-platform) deployment. To maximize the scientific lossy compression ratio on GPUs, achieving minimal information redundancy while preserving the usability of the whole compression framework, as cuSZ-Hi does, we need a new solution for the lossless pipeline, which will be detailed step-by-step in the next.

**Table 1: The NVIDIA Bitcomp compression ratio on the compressed data from different error-bounded lossy compressors (NYX [39] dataset, error bound = 1e-2).**

compressor	Bitcomp CR on comp'ed data	compressor	Bitcomp CR on comp'ed data
cuSZ-Hi-CR	1.03	cuSZ-L	2.37
cuSZ-Hi-TP	1.06	cuSZp2	3.33
cuSZ-I (w/o Bitcomp)	9.62	FZ-GPU	3.33

**5.2.1 Minimizing quantization code length.** The first important design detail of cuSZ-Hi lossless pipeline is that, in the integer quantization code sequence, each value has been resized to the minimized one-byte-width, processed in the uint8\_t format (the out-of-range outliers will be collected and stored separately). Different from other scientific lossy compressors that quantize data offsets [20, 21] or inaccurate extrapolation errors [45], interpolation-based data compressors usually produce quantization codes with a highly-concentrated distribution, including very few large values [36]. Consequently, applying a short data format to store the quantization codes will accelerate the encoding speed and simplify bit patterns without high overheads for recording outliers.

**5.2.2 Investigation and benchmarking of lossless encoders.** To figure out the best-fit lossless pipeline for encoding the cuSZ-Hi quantization codes, we conduct a systematic benchmarking of compressing them with a large variety of GPU-based numerical data encoders introduced in existing works [8, 11]. The LC framework [8] integrates a large variety of lossless encoding algorithms and modules. It can search for and combine existing transforming and reducing components to form synthetic lossless pipelines with a customizable number of stages. NVIDIA nvCOMP [2] includes a series of NVIDIA-proprietary GPU-optimized implementations of lossless compression algorithms. GPULZ [49] is an open-source implementation of the LZSS algorithm for GPUs. ndzip [25] is an open-source high-throughput lossless compressor that supports multi-dimensional data and is compatible with both GPU and CPU architectures.

In our benchmarking, the evaluated lossless pipelines are collected as follows: First, incorporating Huffman encoding as a "preprocessor" in the lossless compression pipeline has been a widely adopted scheme in existing compressors [29, 34, 36], so in addition to the standalone lossless modules, we also include a set of Huffman-incorporated variants corresponding to each of them. Second, for the LC framework, we perform preliminary experiments on several datasets and select 8

representative and adaptive pipelines (RRE1, RRE1-RRE2, etc. as shown in Figure 6) with 1/2/3/4 stages (as indicated by Figure 6, pipelines with more stages are not necessary). The benchmarking is conducted on 4 scientific datasets [51] on a computing platform facilitated with NVIDIA RTX 6000 Ada GPUs.

The compression ratio and overall (compression-decompression) throughput of each lossless pipeline are shown in Figure 6, with Pareto frontiers marked (solutions with throughput less than 25 GiB/s are not included in the frontiers because they bring unacceptable time overheads to the full compression pipeline). Regarding open-source solutions with acceptable compression throughput, we find that the combination of **Huffman encoding** and the **RRE4-TCMS8-RZE1** pipeline achieves high compression ratios on cuSZ-Hi quantization codes. The Zstd [12] compressor in NVIDIA nvCOMP achieves the highest compression ratio. However, not only is this implementation NVIDIA-proprietary, but it also consists of multiple self-contained encoders with coarse component configuration granularity. Consequently, its throughput is significantly low in most scenarios, making it impractical for cuSZ-Hi. The nvCOMP::ANS/Bitcomp and GPULZ may present decent compression ratios in some scenarios, but they show no advantages over the multi-stage LC pipelines. The GDeflate/LZ4/ndzip/Huffman-only lossless solutions exhibit very poor compression ratios and/or throughputs, being infeasible for cuSZ-Hi usage.

According to the benchmarking results and analysis, we adopt the **HF-RRE4-TCMS8-RZE1** lossless pipeline in cuSZ-Hi, forming its compression-ratio-preferred mode, **cuSZ-Hi-CR**. However, Huffman encoding on GPUs also brings a performance bottleneck in the compression framework and lowers the overall compression throughput [41]. To this end, regarding Figure 6, cuSZ-Hi integrates an alternative Huffman-encoding-free lossless pipeline, which is the **TCMS1-BIT1-RRE1** pipeline with high throughput and decent compression ratio. In Section 6, we will see that, cuSZ-Hi with this lossless pipeline (the throughput-preferred **cuSZ-Hi-TP**) also gains very acceptable compression ratios with significantly improved compression throughputs, proving its practical usability.

**5.2.3 The design details of cuSZ-Hi lossless pipelines.** Figure 7 illustrates the two selective lossless pipelines employed in cuSZ-Hi (compressing quantization codes with **Huffman-RRE4-TCMS8-RZE1** pipeline or **TCMS1-BIT1-RRE1** pipeline). The numbers in the module names indicate the per-symbol byte widths. In the Huffman-RRE4-TCMS8-RZE1 pipeline, after the Huffman encoding, RRE4 introduces a bitmap to mark (set to 0) and eliminate symbols identical to their predecessors, subsequently compressing the bitmap recursively. Following this, TCMS8 employs a reversible bitwise operation ( $\text{word} \ll 1 \oplus (\text{word} \gg 63)$ ) to convert symbols from two's complement to magnitude-sign representation. Finally, RZE1 compresses the symbols in a manner similar to RRE4 but marks symbols equal to zero. The substantial clustering zeros produced by Huffman encoding, combined with the





more stable **plain** mode on use cases when the outlier mode compression exhibits errors. For our cuSZ-Hi, as previously introduced in Section 5.2, we evaluate two modes of it with different lossless pipelines: **cuSZ-Hi-CR** and **cuSZ-Hi-TP**.

**6.1.3 Evaluation datasets.** cuSZ-Hi and the baselines are evaluated on 6 real-world scientific datasets (detailed in Table 3). Those datasets are from diverse scientific domains and sources [28, 29, 51], and are widely adopted as representative scientific error-bounded lossy compression benchmarks [26, 30, 34, 36, 50, 51].

**Table 3: Information of the datasets in experiments**

<b>CESM-ATM</b> [22]: Community Earth System Model (Atmosphere).			
79 files	dim: $1800_y \times 3600_x$		total: 1.5 GiB
<b>JHTDB</b> [28]: numerical simulation of turbulence.			
10 files	dim: $512_z \times 512_y \times 512_x$		total: 5 GiB
<b>Miranda</b> [1]: hydrodynamics simulation.			
7 files	dim: $256_z \times 384_y \times 384_x$		total: 1 GiB
<b>Nyx</b> [39]: cosmological hydrodynamics simulation.			
6 files	dim: $512_z \times 512_y \times 512_x$		total: 3.1 GiB
<b>QMCpack</b> [24]: Monte Carlo quantum simulation.			
1 files	dim: $288 \times 115_z \times 69_y \times 69_x$		total: 612 MiB
<b>RTM</b> [23]: reverse time migration for seismic imaging.			
37 files	dim: $449_z \times 449_y \times 235_x$		total: 6.5 GiB

**6.1.4 Evaluation metrics.** Our evaluation metrics are as follows:

- **Fixed-error-bound compression ratio:** We compare the compression ratio (CR) of different compressors on the same data under fixed error bounds. CR is the original input size divided by the compressed size. All error bounds  $eb$  in our evaluations are the value-range-based relative error bound, equivalent to a uniform absolute error bound  $\epsilon$  (in Eq. 1) that equals  $eb$  divided by the input data value range.
- **Rate-distortion:** We plot the compression bit rate and the decompression data PSNR for compressors. The bit rate  $b$  is the average of bits in the compressed data for each input element (i.e.,  $32 \times$  the reciprocal of CR). PSNR [43] measures the difference between the input data and decompressed data via value range and mean-square error, and a higher PSNR is better.
- **Throughput:** Compression and decompression throughput of all the compressors in GiB/s.
- **Fixed-CR visualization:** The visual qualities of the reconstructed data from all the compressors at the same CR.

## 6.2 Evaluation results

**6.2.1 Compression ratio assessment.** Table 4 presents the compression ratios that cuSZ-Hi (2 modes, the compression ratio (CR) preferred mode and the throughput (TP) preferred mode) and 5 baselines achieved on all the evaluated datasets with different error bounds (cuZFP is not covered because it doesn't support fixed-error-bound mode). In almost all test cases, cuSZ-Hi exhibits the best compression ratio, mainly with the CR-preferred mode. In certain cases under large error bounds, the CR can be extremely high (over 300), and the Huffman tree itself can be non-negligible overhead in

**Table 4: Evaluation of compression ratio (CR).** The top 3 CRs per row are shaded in dark blue, light blue, and gray. The last column shows cuSZ-Hi CR improvement over the baselines.

Dataset	$eb$	cuSZ-Hi -CR	cuSZ-Hi -TP	cuSZ-L	cuSZ-1	cuSZ-IB	cuSZp2	FZGPU	max (cuSZ-Hi)	max (Baseline)	adv. percent.
CESM-ATM	1e-2	120.4	210.7	22.6	17.5	70.3	19.2	21.7	210.7	70.3	200%
	1e-3	37.7	40.0	17.4	15.1	30.1	12.8	13.0	40.0	30.1	33%
	1e-4	12.7	13.2	10.0	10.0	14.0	7.9	7.7	13.2	14.0	-6%
JHTDB	1e-2	402.1	364.2	26.5	29.2	128.2	14.3	12.1	402.1	128.2	214%
	1e-3	63.6	47.5	17.6	25.2	34.6	9.8	9.9	63.6	34.6	84%
	1e-4	15.0	12.0	10.7	13.3	13.3	5.0	6.4	15.0	13.3	13%
MIRANDA	1e-2	424.9	520.9	26.9	28.3	163.5	30.4	30.6	520.9	163.5	219%
	1e-3	129.3	118.0	22.8	26.1	75.1	16.6	19.2	129.3	75.1	72%
	1e-4	39.2	37.0	15.2	19.4	33.8	10.1	11.8	39.2	33.8	16%
NYX	1e-2	823.5	837.1	30.1	29.5	249.0	28.1	25.3	837.1	249.0	236%
	1e-3	123.1	88.5	23.8	27.9	65.2	17.3	14.4	123.1	65.2	89%
	1e-4	23.7	17.4	15.2	18.7	25.0	8.4	8.4	23.7	25.0	-6%
QMCpack	1e-2	570.6	497.5	28.5	29.2	163.5	23.6	19.0	570.6	163.5	249%
	1e-3	169.2	135.1	20.9	27.6	77.1	13.3	12.1	169.2	77.1	120%
	1e-4	49.8	41.9	14.8	22.5	34.2	7.3	8.3	49.8	34.2	46%
RTM	1e-2	618.7	775.1	28.6	28.6	227.8	44.2	32.0	775.1	227.8	240%
	1e-3	165.8	146.3	24.6	27.2	94.7	23.6	20.9	165.8	94.7	75%
	1e-4	44.0	38.2	17.6	21.4	45.0	12.6	12.2	44.0	45.0	-2%

the compressed data so that the TP-preferred mode without Huffman encoding may have a higher compression ratio than the CR-preferred mode. With synthetical design updates on both the interpolation module and lossless pipeline, cuSZ-Hi successfully gains the compression ratio improvements over baselines ( $> 200\%$  for 6/18 cases,  $> 50\%$  for 11/18 cases), empowering optimized data size reduction over different error-bound constraints. Additionally, it is worth noticing that, as the state-of-the-art compressor in terms of compression ratio, cuSZ-IB relies on NVIDIA-proprietary components. When only compared with non-proprietary solutions, the open-source cuSZ-Hi can achieve much higher CR improvements, ranging from 113% to 2786% in all test cases.

**6.2.2 Rate-distortion assessment.** Besides the compression ratio discussed in Section 6.2.1, in most scientific lossy compression use cases, the decompression data quality is also critical for justifying the compression solution's usability. Regarding a joint assessment of compression ratio and data quality, we profile the PSNR metric of decompressed data from different compressors and plot their rate-distortion curves in Figure 8. For each dataset, the upper rectangle plot shows a full bitrate range for all baselines, and the lower square plot demonstrates a narrow bitrate range to visualize better the rate-distortion of high-ratio compressor cuSZ-Hi and cuSZ-I(B). Among all datasets, The CR-preferred mode of cuSZ-Hi (cuSZ-Hi-CR) has delivered stable and excellent rate-distortion, achieving the best compression ratio on most data PSNR value. For example, on the Miranda dataset, cuSZ-Hi-CR achieves  $\approx 140\%$ 120% compression ratio improvement over the best baseline cuSZ-IB when the decompression data PSNR is around 59/63. For compressing the QMCpack dataset, with the decompression data PSNR fixed around 60/76, cuSZ-Hi-CR achieves  $\approx 215\%$ 80% compression

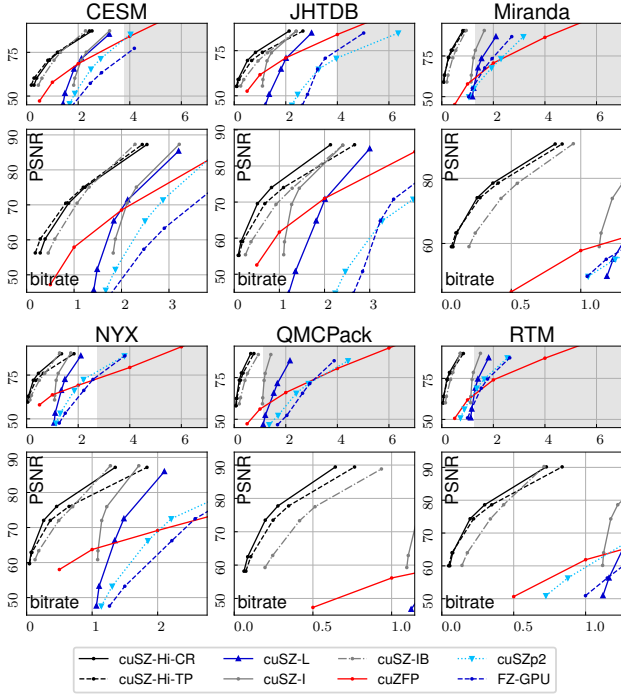
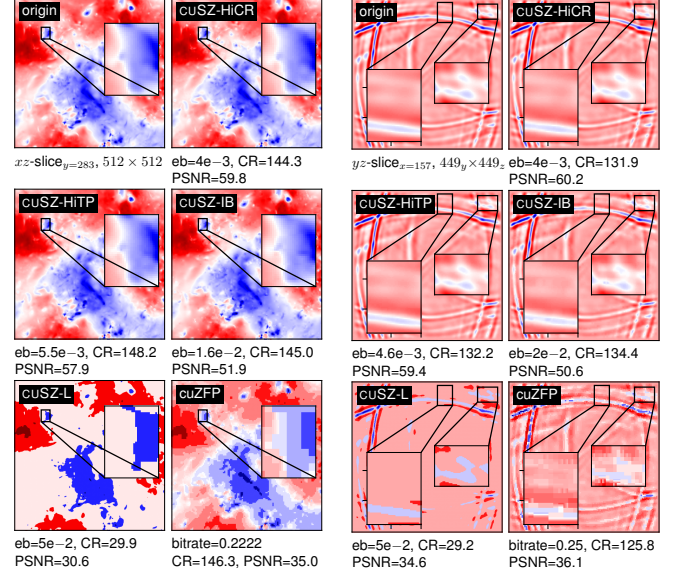


**Figure 8: Rate distortion assessment: global (top) and local (bottom) for each dataset. The highly compressible (low-bitrate) regions are indicated by white canvases on top and are zoomed out on bottom.**

ratio improvement over cuSZ-IB. Moreover, The throughput-preferred mode of cuSZ-Hi (cuSZ-Hi-TP) presents excellent rate-distortion as well, exhibiting close decomposition data quality to cuSZ-Hi-CR and outperforming the best baseline (cuSZ-IB) in many cases. Given the fact that cuSZ-Hi-TP has a higher throughput than both cuSZ-IB and cuSZ-Hi-CR (detailed in Section 6.2.4), it can become a top compression solution for performance-sensitive use tasks, such as in-time streaming data compression and so on.

**6.2.3 Visualization assessment.** In this subsection, we present several detailed showcases of high-quality cuSZ-Hi compression, visualizing the decomposition data from different compressors under the fixed compression ratio. Figure 9 presents 2 series of visualization results on 2 data snapshots (JHTDB-pressure-#2500 and RTM-#3600), including the slice visualization of the original data and multiple decompression results from cuSZ-Hi and baselines (some baselines are omitted from the visualizations as they have very limited compression ratio and/or data quality), with the compression ratios aligned to close values (e.g.  $\approx 144$  for JHTDB). In each case, in similar compression ratios, when obvious error artifacts appear in the decompression data from baselines (cuSZ-IB, cuSZ-L, and cuZFP), the decompression data of cuSZ-Hi shows the best visualization quality without significant distortions and artifacts from the original data. With the evaluation of both

data PSNR and visual quality, we have all-roundly verified the high compression fidelity of cuSZ-Hi.



**(a) JHTDB #2500 (b) RTM #3600**  
**Figure 9: Visualization for quality evaluation.**

**6.2.4 Speed assessment.** After verifying the excellent compression ratio and data quality of cuSZ-Hi, we also evaluate its efficiency, proving that cuSZ-Hi exhibits competitive compression throughput among high-ratio GPU-based scientific lossy compressors. After profiling the computing throughput (in terms of GPU kernel speed) of several scientific lossy compressors on 2 GPU platforms (NVIDIA A100 and RTX 6000 Ada), we present the results acquired in Figure 10. As cuZFP, cuSZp2, and FZ-GPU are throughput-oriented compressors with limited compression ratios, it is natural that cuSZ-Hi features relatively lower throughput than them. When we focus the comparison on compressors that can deliver decent compression ratio and quality, we can notice that cuSZ-Hi has comparable (for CR-preferred mode) or better (for TP-preferred mode) throughput than cuSZ-L and cuSZ-I(B). On NVIDIA RTX6000 Ada, attributed to its high FP computational power and cache capacity, cuSZ-Hi-CR shows a similar compression speed and an acceptable  $\sim 20\%$  decompression time overhead compared to cuSZ-I(B) when achieving quite higher compression ratios. On NVIDIA A100, the compression/decompression overhead of cuSZ-Hi-CR compared to cuSZ-I(B) is also mostly limited within  $\sim 25\%$ . Additionally, while the compression ratio and data quality of cuSZ-Hi-TP is still better than any baselines, it exhibits a throughput constantly higher than cuSZ-I(B), even outperforming cuSZ-L on NVIDIA Ada 6000, showing  $\approx 20\% \sim 40\%$  speed improvement over cuSZ-L (also up to doubled compression speed of cuSZ-I(B)) on both compression and decompression. In conclusion, the satisfactory throughput of cuSZ-Hi successfully guarantees its usability in high-performance scientific computing and data management tasks. Moreover, users can adaptively select either of its two modes, depending on their

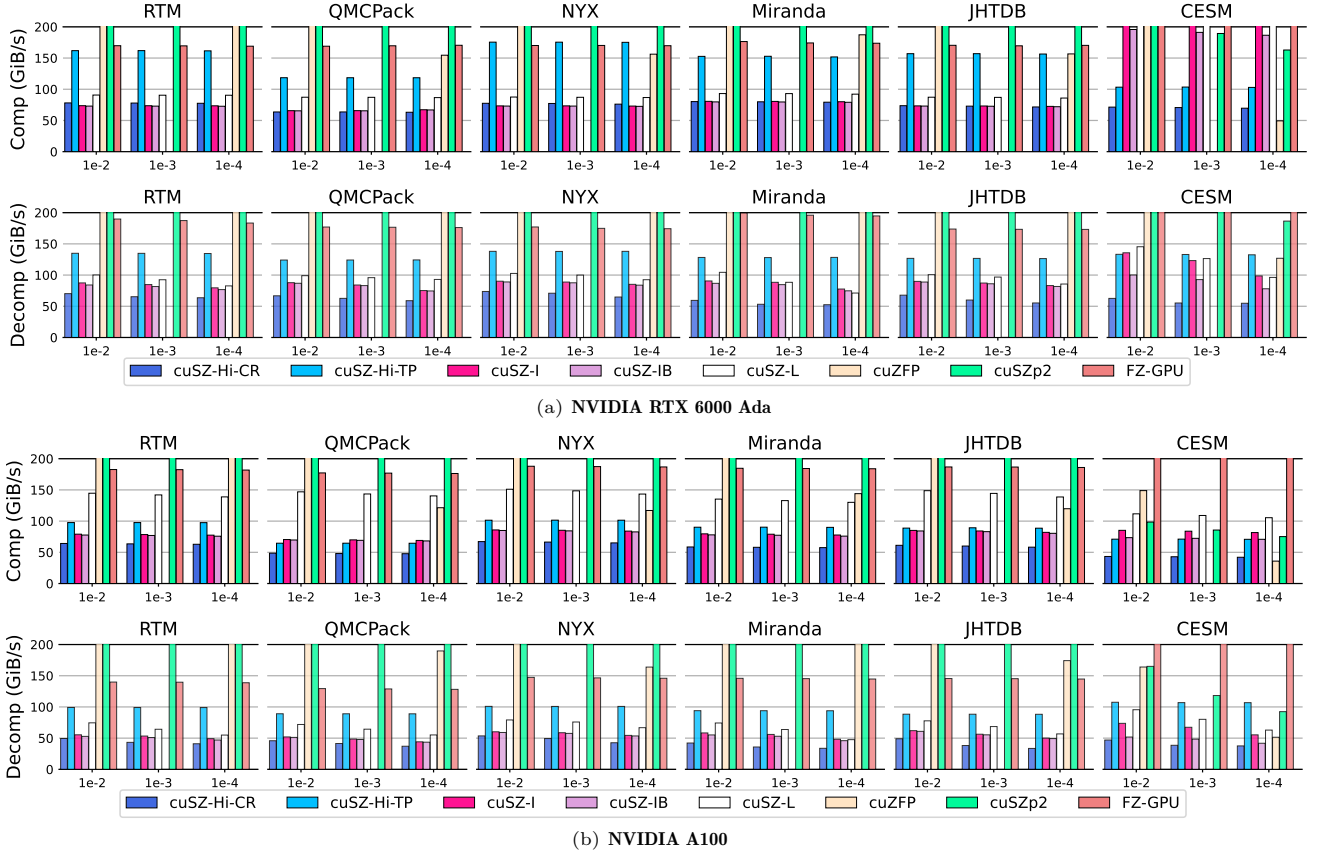


Figure 10: Compression and decompression speed in GiB/s on NVIDIA Ada RTX 6000 and A100 with different error bounds. The cuZFP speeds are presented when cuZFP achieves comparable PSNR, or are hidden if no matching PSNR can be found.

preference for optimizing compression ratio or computing throughput.

**6.2.5 Ablation study.** At the end of our evaluation, we would like to justify the effectiveness of the newly proposed design components in cuSZ-Hi with a systematic ablation study. To this end, besides the complete framework of cuSZ-Hi and the baseline cuSZ-IB, we also evaluated several incremental frameworks of cuSZ-IB, stacking separate cuSZ-Hi features. Those results are reported in Table 5, which include the compression ratios of the aforementioned compression frameworks on 4 datasets. Specifically, revising the data partition and anchor stride can bring 6% ~ 60% compression improvement over the original cuSZ-IB, and further reordering the quantization codes can raise the compression ratio by an additional 6% ~ 55%. Moreover, bringing auto-tuned selection between multi-dimensional and one-dimensional interpolation in the compression framework increases the compression ratio for 8% ~ 19%, and finally, the cuSZ-Hi-CR with optimized lossless encoding pipeline gets a compression ratio which is 16% ~ 50% higher than before. According to Table 5, each design detail described in Section 5 has contributed well to the improvement of cuSZ-Hi compression ratio.

Table 5: Ablation study: compression ratios of cuSZ-IB, cuSZ-Hi, and different design increments between them.

dataset	eb	cuSZ-IB	+new data partition & anchor	+quant code reorder	+MD interp & auto-tune	cuSZ-HiCR
JHTDB	1e-2	128.2	$\xrightarrow{+23\%}$ 158.2 (so far) 1.23 $\times$	$\xrightarrow{+46\%}$ 230.9 (so far) 1.80 $\times$	$\xrightarrow{+17\%}$ 270.2 (so far) 2.11 $\times$	$\xrightarrow{+49\%}$ 402.1 FINALLY 3.14 $\times$
	1e-3	34.6	$\xrightarrow{+6\%}$ 36.8 (so far) 1.06 $\times$	$\xrightarrow{+10\%}$ 40.6 (so far) 1.17 $\times$	$\xrightarrow{+15\%}$ 46.6 (so far) 1.35 $\times$	$\xrightarrow{+36\%}$ 63.6 FINALLY 1.84 $\times$
Miranda	1e-2	163.5	$\xrightarrow{+35\%}$ 220.2 (so far) 1.35 $\times$	$\xrightarrow{+32\%}$ 290.8 (so far) 1.78 $\times$	$\xrightarrow{+19\%}$ 345.5 (so far) 2.11 $\times$	$\xrightarrow{+23\%}$ 424.9 FINALLY 2.60 $\times$
	1e-3	75.1	$\xrightarrow{+13\%}$ 84.6 (so far) 1.13 $\times$	$\xrightarrow{+6\%}$ 89.9 (so far) 1.20 $\times$	$\xrightarrow{+15\%}$ 103.3 (so far) 1.38 $\times$	$\xrightarrow{+25\%}$ 129.3 FINALLY 1.72 $\times$
NYX	1e-2	249.0	$\xrightarrow{+59\%}$ 395.1 (so far) 1.59 $\times$	$\xrightarrow{+26\%}$ 496.8 (so far) 2.00 $\times$	$\xrightarrow{+13\%}$ 561.4 (so far) 2.25 $\times$	$\xrightarrow{+47\%}$ 823.5 FINALLY 3.31 $\times$
	1e-3	65.2	$\xrightarrow{+12\%}$ 72.9 (so far) 1.12 $\times$	$\xrightarrow{+8\%}$ 78.4 (so far) 1.20 $\times$	$\xrightarrow{+9\%}$ 85.1 (so far) 1.31 $\times$	$\xrightarrow{+45\%}$ 123.1 FINALLY 1.89 $\times$
RTM	1e-2	227.8	$\xrightarrow{+36\%}$ 309.9 (so far) 1.36 $\times$	$\xrightarrow{+55\%}$ 480.3 (so far) 2.11 $\times$	$\xrightarrow{+13\%}$ 541.7 (so far) 2.38 $\times$	$\xrightarrow{+14\%}$ 618.7 FINALLY 2.72 $\times$
	1e-3	94.7	$\xrightarrow{+14\%}$ 107.6 (so far) 1.14 $\times$	$\xrightarrow{+11\%}$ 119.7 (so far) 1.26 $\times$	$\xrightarrow{+10\%}$ 131.4 (so far) 1.39 $\times$	$\xrightarrow{+26\%}$ 165.8 FINALLY 1.75 $\times$

## 7 Conclusion

Scientific error-bounded lossy compression is an essential technique for exascale scientific data management. Unfortunately,

as fast-evolving GPUs play a more and more important role in scientific supercomputing, existing scientific error-bounded lossy compression toolkits on GPU platforms are still immature and sub-optimal. This paper proposes cuSZ-Hi, the first GPU-based high-ratio, high-quality, and open-source scientific error-bounded lossy compressor. Integrating highly advanced and GPU-customized data interpolation schemes and also fine-tuned lossless encoding pipelines, cuSZ-Hi significantly outperforms state-of-the-art GPU-based scientific lossy compressors. When exhibiting close or better throughput than the state-of-the-art high-ratio GPU-based compressor cuSZ-I that facilitates NVIDIA-proprietary encoding module, cuSZ-Hi can significantly improve its compression ratio by up to 200% in the same compression task. In the future, we will improve cuSZ-Hi in the following aspects: 1) Reduce the interpolation computing overhead on GPU platforms; 2) Explore and design better lossless encoders for quantization codes; 3) Enhance the flexibility of compression, such as develop an auto-selection mechanism for different data compressor archetypes and/or lossless pipelines to dynamically fit different data characteristics and compression requirements.

## 8 Acknowledgments

This research was supported by the U.S. Department of Energy, Office of Science, Advanced Scientific Computing Research (ASCR), under contracts DE-AC02-06CH11357. This work was also supported by the National Science Foundation (Grant Nos. 2104023, 2311875, 2344717).

## References

- [1] [n.d.]. *Miranda application*. <https://wci.llnl.gov/simulation/computer-codes/miranda>
- [2] [n.d.]. *nvCOMP*. <https://github.com/NVIDIA/nvcomp>.
- [3] 2021. NERSC Perlmutter - Lawrence Berkeley National Laboratory. <https://docs.nersc.gov/systems/perlmutter/architecture/>.
- [4] 2022. Frontier - Oak Ridge Leadership Computing Facility. <https://www.olcf.ornl.gov/frontier/>.
- [5] 2023. El Capitan: NNSA's first exascale machine. <https://asc.llnl.gov/exascale/el-capitan>.
- [6] 2024. Aurora - Argonne Leadership Computing Facility. <https://www.alcf.anl.gov/aurora>.
- [7] Mark Ainsworth, Ozan Tugluk, Ben Whitney, and Scott Klasky. 2018. Multilevel techniques for compression and reduction of scientific data—the univariate case. *Computing and Visualization in Science* 19, 5 (2018), 65–76.
- [8] Noushin Azami, Alex Fallin, and Martin Burtcher. 2025. Efficient Lossless Compression of Scientific Floating-Point Data on CPUs and GPUs. In *Proceedings of the 30th ACM International Conference on Architectural Support for Programming Languages and Operating Systems, Volume 1* (Rotterdam, Netherlands) (ASPLOS '25). Association for Computing Machinery, New York, NY, USA, 395–409. <https://doi.org/10.1145/3669940.3707280>
- [9] Rafael Ballester-Ripoll, Peter Lindstrom, and Renato Pajarola. 2019. TTHRESH: Tensor compression for multidimensional visual data. *IEEE transactions on visualization and computer graphics* 26, 9 (2019), 2891–2903.
- [10] David Carrasco-Busturia, Emiliano Ippoliti, Simone Meloni, Ursula Rothlisberger, and Jógvan Magnus Haugaard Olsen. 2024. Multiscale biomolecular simulations in the exascale era. *Current Opinion in Structural Biology* 86 (2024), 102821. <https://doi.org/10.1016/j.sbi.2024.102821>
- [11] Xinyu Chen, Jiannan Tian, Ian Beaver, Cynthia Freeman, Yan Yan, Jianguo Wang, and Dingwen Tao. 2024. FCBench: Cross-Domain Benchmarking of Lossless Compression for Floating-Point Data. *Proceedings of the VLDB Endowment* 17, 6 (2024), 1418–1431.
- [12] Yann Collet. 2015. Zstandard – Real-time data compression algorithm. <http://facebook.github.io/zstd/> (2015).
- [13] cuZFP. 2020. [https://github.com/LLNL/zfp/tree/develop/src/cuda\\_zfp](https://github.com/LLNL/zfp/tree/develop/src/cuda_zfp). Online.
- [14] L Peter Deutsch. 1996. GZIP file format specification version 4.3.
- [15] Peter Deutsch. 1996. *DEFLATE compressed data format specification version 1.3*. Technical Report.
- [16] Qian Gong, Jieyang Chen, Ben Whitney, Xin Liang, Viktor Reshniak, Tania Banerjee, Jaemoon Lee, Anand Rangarajan, Lipeng Wan, Nicolas Vidal, Qing Liu, Ana Gainaru, Norbert Podhorszki, Richard Archibald, Sanjay Ranka, and Scott Klasky. 2023. MGARD: A multigrid framework for high-performance, error-controlled data compression and refactoring. *SoftwareX* 24 (2023), 101590. <https://doi.org/10.1016/j.softx.2023.101590>
- [17] Lucas Hayne, John Clyne, and Shaomeng Li. 2021. Using Neural Networks for Two Dimensional Scientific Data Compression. In *2021 IEEE International Conference on Big Data (Big Data)*. IEEE, 2956–2965.
- [18] Jiajun Huang, Sheng Di, Xiaodong Yu, Yujia Zhai, Jinyang Liu, Zizhe Jian, Xin Liang, Kai Zhao, Xiaoyi Lu, Zizhong Chen, Franck Cappello, Yanfei Guo, and Rajeev Thakur. 2024. hZCCL: Accelerating Collective Communication with Co-Designed Homomorphic Compression. In *SC24: International Conference for High Performance Computing, Networking, Storage and Analysis*. 1–15. <https://doi.org/10.1109/SC41406.2024.00110>
- [19] Langwen Huang and Torsten Hoefer. 2022. Compressing multidimensional weather and climate data into neural networks. *arXiv preprint arXiv:2210.12538* (2022).
- [20] Yafan Huang, Sheng Di, Guanpeng Li, and Franck Cappello. 2024. cuSZp2: A GPU Lossy Compressor with Extreme Throughput and Optimized Compression Ratio. In *SC24: International Conference for High Performance Computing, Networking, Storage and Analysis*. IEEE, 1–18.
- [21] Yafan Huang, Sheng Di, Xiaodong Yu, Guanpeng Li, and Franck Cappello. 2023. cuSZp: An Ultra-fast GPU Error-bounded Lossy Compression Framework with Optimized End-to-End Performance. In *Proceedings of the International Conference for High Performance Computing, Networking, Storage and Analysis*. 1–13.

- [22] J. E. Kay and et al. 2015. The Community Earth System Model (CESM) large ensemble project: A community resource for studying climate change in the presence of internal climate variability. *Bulletin of the American Meteorological Society* 96, 8 (2015), 1333–1349.
- [23] Suha Kayum et al. 2020. GeoDRIVE – a high performance computing flexible platform for seismic applications. *First Break* 38, 2 (2020), 97–100.
- [24] Jeongnim Kim et al. 2018. QMCPACK: an open source ab initio quantum Monte Carlo package for the electronic structure of atoms, molecules and solids. *Journal of Physics: Condensed Matter* 30, 19 (2018), 195901. <https://doi.org/10.1088/1361-648x/aab9c3>
- [25] Fabian Knorr, Peter Thoman, and Thomas Fahringer. 2021. ndzip-gpu: efficient lossless compression of scientific floating-point data on GPUs. In *Proceedings of the International Conference for High Performance Computing, Networking, Storage and Analysis*. 1–14.
- [26] Shaomeng Li, Peter Lindstrom, and John Clyne. 2023. Lossy scientific data compression with SPERR. In *2023 IEEE International Parallel and Distributed Processing Symposium (IPDPS)*. IEEE, 1007–1017.
- [27] Xiao Li, Jaemoon Lee, Anand Rangarajan, and Sanjay Ranka. 2024. Attention Based Machine Learning Methods for Data Reduction with Guaranteed Error Bounds. In *2024 IEEE International Conference on Big Data (BigData)*. 1039–1048. <https://doi.org/10.1109/BigData62323.2024.10825655>
- [28] Yi Li, Eric Perlman, Minping Wan, Yunke Yang, Charles Meneveau, Randal Burns, Shiyi Chen, Alexander Szalay, and Gregory Eyink. 2008. A public turbulence database cluster and applications to study Lagrangian evolution of velocity increments in turbulence. *Journal of Turbulence* 9 (2008), N31.
- [29] Xin Liang, Kai Zhao, Sheng Di, Sihuan Li, Robert Underwood, Ali M. Gok, Jiannan Tian, Junjing Deng, Jon C. Calhoun, Dingwen Tao, Zizhong Chen, and Franck Cappello. 2023. SZ3: A Modular Framework for Composing Prediction-Based Error-Bounded Lossy Compressors. *IEEE Transactions on Big Data* 9, 2 (2023), 485–498. <https://doi.org/10.1109/TBDATA.2022.3201176>
- [30] Peter Lindstrom. 2014. Fixed-rate compressed floating-point arrays. *IEEE transactions on visualization and computer graphics* 20, 12 (2014), 2674–2683.
- [31] Jinyang Liu, Sheng Di, Sian Jin, Kai Zhao, Xin Liang, Zizhong Chen, and Franck Cappello. 2023. Scientific Error-bounded Lossy Compression with Super-resolution Neural Networks. In *2023 IEEE International Conference on Big Data (BigData)*. IEEE, 229–236.
- [32] Jinyang Liu, Sheng Di, Kai Zhao, Sian Jin, Dingwen Tao, Xin Liang, Zizhong Chen, and Franck Cappello. 2021. Exploring Autoencoder-based Error-bounded Compression for Scientific Data. In *2021 IEEE International Conference on Cluster Computing (CLUSTER)*. IEEE, 294–306.
- [33] Jinyang Liu, Sheng Di, Kai Zhao, Xin Liang, Zizhong Chen, and Franck Cappello. 2022. Dynamic quality metric oriented error bounded lossy compression for scientific datasets. In *2022 SC22: International Conference for High Performance Computing, Networking, Storage and Analysis (SC)*. IEEE Computer Society, 892–906.
- [34] Jinyang Liu, Sheng Di, Kai Zhao, Xin Liang, Sian Jin, Zizhe Jian, Jiajun Huang, Shixun Wu, Zizhong Chen, and Franck Cappello. 2024. High-performance effective scientific error-bounded lossy compression with auto-tuned multi-component interpolation. *Proceedings of the ACM on Management of Data* 2, 1 (2024), 1–27.
- [35] Jinyang Liu, Sihuan Li, Sheng Di, Xin Liang, Kai Zhao, Dingwen Tao, Zizhong Chen, and Franck Cappello. 2021. Improving Lossy Compression for SZ by Exploring the Best-Fit Lossless Compression Techniques. In *2021 IEEE International Conference on Big Data (Big Data)*. 2986–2991. <https://doi.org/10.1109/BigData52589.2021.9671954>
- [36] Jinyang Liu, Jiannan Tian, Shixun Wu, Sheng Di, Boyuan Zhang, Robert Underwood, Yafan Huang, Jiajun Huang, Kai Zhao, Guanpeng Li, Dingwen Tao, Zizhong Chen, and Franck Cappello. 2024. CUSZ-i: High-Ratio Scientific Lossy Compression on GPUs with Optimized Multi-Level Interpolation. In *SC24: International Conference for High Performance Computing, Networking, Storage and Analysis*. 1–15. <https://doi.org/10.1109/SC41406.2024.00019>
- [37] Youyuan Liu, Wenqi Jia, Taolue Yang, Miao Yin, and Sian Jin. 2024. Enhancing Lossy Compression Through Cross-Field Information for Scientific Applications. In *SC24-W: Workshops of the International Conference for High Performance Computing, Networking, Storage and Analysis*. 300–308. <https://doi.org/10.1109/SCW63240.2024.00046>
- [38] Yuzhe Lu, Kairong Jiang, Joshua A Levine, and Matthew Berger. 2021. Compressive neural representations of volumetric scalar fields. In *Computer Graphics Forum*, Vol. 40. Wiley Online Library, 135–146.
- [39] NYX simulation. 2019. <https://amrex-astro.github.io/Nyx>. Online.
- [40] William A Pearlman, Asad Islam, Nithin Nagaraj, and Amir Said. 2004. Efficient, low-complexity image coding with a set-partitioning embedded block coder. *IEEE transactions on circuits and systems for video technology* 14, 11 (2004), 1219–1235.
- [41] Cody Rivera, Sheng Di, Jiannan Tian, Xiaodong Yu, Dingwen Tao, and Franck Cappello. 2022. Optimizing Huffman Decoding for Error-Bounded Lossy Compression on GPUs. In *2022 IEEE International Parallel and Distributed Processing Symposium (IPDPS)*. 717–727. <https://doi.org/10.1109/IPDPS53621.2022.00075>
- [42] Dingwen Tao, Sheng Di, Zizhong Chen, and Franck Cappello. 2017. Significantly improving lossy compression for scientific data sets based on multidimensional prediction and error-controlled quantization. In *2017 IEEE International Parallel and Distributed Processing Symposium*. IEEE, 1129–1139.
- [43] Dingwen Tao, Sheng Di, Hanqi Guo, Zizhong Chen, and Franck Cappello. 2019. Z-checker: A framework for assessing lossy compression of scientific data. *The International Journal of High Performance Computing Applications* 33, 2 (2019), 285–303. <https://doi.org/10.1177/1094342017737147>
- [44] Jiannan Tian, Sheng Di, Xiaodong Yu, Cody Rivera, Kai Zhao, Sian Jin, Yunhe Feng, Xin Liang, Dingwen Tao, and Franck Cappello. 2021. cuSZ (x): Optimizing Error-Bounded Lossy Compression for Scientific Data on GPUs. *CoRR* (2021).
- [45] Jiannan Tian, Sheng Di, Kai Zhao, Cody Rivera, Megan Hickman Fulp, Robert Underwood, Sian Jin, Xin Liang, Jon Calhoun, Dingwen Tao, and Franck Cappello. 2020. cuSZ: An Efficient GPU-Based Error-Bounded Lossy Compression Framework for Scientific Data. In *Proceedings of the ACM International Conference on Parallel Architectures and Compilation Techniques* (Virtual Event, GA, USA) (PACT ’20). Association for Computing Machinery, New York, NY, USA, 3–15. <https://doi.org/10.1145/3410463.3414624>
- [46] P.K. Yeung, Kiran Ravikumar, Stephen Nichols, and Rohini Uma-Vaideswaran. 2025. GPU-enabled extreme-scale turbulence simulations: Fourier pseudo-spectral algorithms at the exascale using OpenMP offloading. *Computer Physics Communications* 306 (2025), 109364. <https://doi.org/10.1016/j.cpc.2024.109364>
- [47] Xiaodong Yu, Sheng Di, Kai Zhao, Jiannan Tian, Dingwen Tao, Xin Liang, and Franck Cappello. 2022. SZx: an Ultra-fast Error-bounded Lossy Compressor for Scientific Datasets. *arXiv preprint arXiv:2201.13020* (2022).
- [48] Boyuan Zhang, Jiannan Tian, Sheng Di, Xiaodong Yu, Yunhe Feng, Xin Liang, Dingwen Tao, and Franck Cappello. 2023. FZ-GPU: A Fast and High-Ratio Lossy Compressor for Scientific Computing Applications on GPUs. *arXiv preprint arXiv:2304.12557* (2023).
- [49] Boyuan Zhang, Jiannan Tian, Sheng Di, Xiaodong Yu, Martin Swamy, Dingwen Tao, and Franck Cappello. 2023. GPULZ: Optimizing LZSS Lossless Compression for Multi-byte Data on Modern GPUs. In *Proceedings of the 37th International Conference on Supercomputing*. 348–359.
- [50] Kai Zhao, Sheng Di, Maxim Dmitriev, Thierry-Laurent D. Tonelot, Zizhong Chen, and Franck Cappello. 2021. Optimizing Error-Bounded Lossy Compression for Scientific Data by Dynamic Spline Interpolation. In *2021 IEEE 37th International Conference on Data Engineering (ICDE)*. 1643–1654. <https://doi.org/10.1109/ICDE51399.2021.00145>
- [51] Kai Zhao, Sheng Di, Xin Lian, Sihuan Li, Dingwen Tao, Julie Bessac, Zizhong Chen, and Franck Cappello. 2020. SDRBench: Scientific Data Reduction Benchmark for Lossy Compressors. In *2020 IEEE International Conference on Big Data (Big Data)*. 2716–2724.
- [52] Kai Zhao, Sheng Di, Xin Liang, Sihuan Li, Dingwen Tao, Zizhong Chen, and Franck Cappello. 2020. Significantly Improving Lossy Compression for HPC Datasets with Second-Order Prediction

and Parameter Optimization. In *Proceedings of the 29th International Symposium on High-Performance Parallel and Distributed Computing* (Stockholm, Sweden) (*HPDC '20*). Association for Computing Machinery, New York, NY, USA, 89–100. <https://doi.org/10.1145/3369583.3392688>